International Journal of Heat and Mass Transfer 70 (2014) 779–792

Contents lists available at ScienceDirect

International Journal of Heat and Mass Transfer

journal homepage: www.elsevier.com/locate/ijhmt

Scaling properties of the equation for passive scalar transport in wall-bounded turbulent flows

S. Saha [a,*], J.C. Klewicki [a,b], A.S.H. Ooi [a], H.M. Blackburn [c], T. Wei [d]

[a] Department of Mechanical Engineering, University of Melbourne, Melbourne, VIC 3010, Australia
[b] Department of Mechanical Engineering, University of New Hampshire, Durham, NH 03824, USA
[c] Department of Mechanical and Aerospace Engineering, Monash University, VIC 3800, Australia
[d] Department of Mechanical Engineering, New Mexico Institute of Mining and Technology, Socorro, NM 87801, USA

ARTICLE INFO

Article history:
Received 25 June 2013
Received in revised form 8 November 2013
Accepted 17 November 2013

Keywords:
Turbulent channel flow
Heat transfer
Prandtl number
Reynolds number
Scaling

ABSTRACT

Data from direct numerical simulations (DNS) of fully-developed turbulent channel flows subjected to a constant surface heat-flux are used to explore the scaling behaviours admitted by the mean thermal energy equation. Following the framework of Wei et al. (2005) [1,2], the analysis employs a theory based on the magnitude ordering of terms in the mean thermal energy equation of wall-bounded turbulent heat transfer. A four layer thermal structure has been identified from the leading order terms in the mean energy equation. A review of the limitations of traditional and existing scaling of mean temperature and turbulent heat flux is conducted. The possibilities of a new scaling approach with the introduction of generalized thermal length scale are discussed within the context of the four-layer framework. This methodology generally seeks to determine the invariant form(s) admitted by the relevant equation. Investigation of normalized statistical quantities applicable to inner, outer and intermediate regions of the flow, whose properties are dependent on a small parameter that is a function of either Reynolds number or both Reynolds and Prandtl numbers, shows inconsistencies between the normalizations on the different subdomains. Although the present scaling approach successfully explores the generalized properties of intermediate layer, issues pertaining to simultaneously and self-consistently reconciling the inner and intermediate normalizations remain unresolved.

1. Introduction

Wall-bounded turbulent flows are present in numerous industrial, technological, aerospace and naval applications that involve heat and mass transport. The knowledge of the mean temperature profile is generally essential, and a number of approaches have been attempted to predict the variation of this scalar field over the flow domain. Based on the Reynolds analogy between momentum and scalar transport, many researchers have employed approaches that effectively assume 'the law of wall' [3–5]. This approach supposes that the mean temperature and turbulent heat flux profiles become invariant when the viscous or inner scaled distance from the wall is employed. Conveniently, one may then apply this form of the 'Reynolds analogy' to relate the eddy viscosity to the eddy thermal diffusivity. A brief review of the many variations of this approach are listed by Dhotre and Joshi [6]. Such approaches also naturally embrace the use of higher order closures for the Reynolds averaged momentum and heat balance equations. Although these kinds of models are fast and amenable to use at very high Reynolds and Prandtl numbers, the correct estimation of mean quantities critically depends on the accurate determination of the appropriate normalizations and the length, velocity and temperature scales they employ. Earlier investigations showed that the normalized mean temperature only exhibits slight variations due to the Reynolds number [7,8]. Temperature profiles, however, are seen to change much more rapidly with varying Prandtl number, both in turbulent channel [7] and pipe [9] flow. To date, the combined effects of Reynolds and Prandtl numbers have not been systematically investigated in the context of the underlying transport equation. It is important, however, to understand how the thermal transport equation can be cast into invariant forms that properly reflect the dominant physical mechanism, as this reveals the effects of the governing parameters on the thermal field statistics.

Traditional representations of temperature and turbulent heat flux profiles generally employ either inner or outer normalizations. These normalizations, however, fail to provide invariant profiles as the relevant non-dimensional parameters are varied [7–25]. Moreover, neither of these normalization are successful in

* Corresponding author. Tel.: +61 3 8344 6748; fax: +61 3 8344 4290.
E-mail addresses: sumons@student.unimelb.edu.au (S. Saha), klewicki@unimelb.edu.au (J.C. Klewicki), aooi@unimelb.edu.au (A.S.H. Ooi), hugh.blackburn@eng.monash.edu.au (H.M. Blackburn), twei@nmt.edu (T. Wei).

0017-9310/$ - see front matter © 2013 Elsevier Ltd. All rights reserved.
http://dx.doi.org/10.1016/j.ijheatmasstransfer.2013.11.057

the vicinity of the peak turbulent heat flux profiles. Inner normalization of the mean temperature uses the so-called friction temperature, and the wall distance is normalized by the friction velocity and the kinematic viscosity. This normalization, however, is traditionally relevant over a small region adjacent to the wall, the conductive sublayer [4], whose width varies as a function of Prandtl number. Furthermore, the data from the logarithmic layer for temperature exhibit different mean temperature profiles as a function of both Reynolds and Prandtl numbers. This range of phenomena is richer than exhibited by the momentum field. It arises from the additional parameter, Prandtl number.

In order to understand the underlying physics of heat transfer in turbulent flows for moderate to high Reynolds and Prandtl numbers, dimensional and similarity analysis play central roles. In this regard, the literature is extensive, and thus here we only discuss a subset of recent findings. Wang et al. [5] introduced the temperature scaling for forced convection turbulent boundary layers using a variant of the similarity theory by George and Castillo [26]. A power law was found for the temperature profile in an intermediate region, and this melds into a composite profile in the wake and near-wall regions. Apart from dimensional analysis or similarity analysis, Churchill and Chan [27] and Churchill et al. [28] introduced a new approach by proposing an algebraic model to predict the mean temperature profile from a knowledge of the velocity profile and the turbulent Prandtl number. Using the model of Churchill and Chan [27] and Churchill et al. [28], Le and Papavassiliou [29] developed a temperature profile for low Reynolds number turbulent flow. But they pointed out the limitation of the theoretical predictions by Churchill and co-workers at very high Prandtl numbers. Marati et al. [30] derived the symmetry invariant mean profiles for a passive scalar in wall-bounded turbulent flow based on the symmetry properties of the Navier–Stokes equation and the energy equation. Their results showed the validation of the well-known logarithmic laws as well as interpreted linear, algebraic and exponential profiles in different physical regimes.

Building upon his initial studies indicating the existence of an intermediate layer (mesolayer), Afzal [31] employed a different approach to investigate the properties of the mean momentum and thermal balance in fully developed turbulent channel flow having both smooth and transitionally rough surfaces. Seena and Afzal [32] proposed a power law temperature distribution for a fully developed turbulent channel flow for large Peclet numbers (product of Reynolds and Prandtl numbers). They supposed that both the mean turbulent flow and thermal fields were divided into inner and outer layers. The matching of the velocity profile by the Isakson–Millikan–Kolmogorov hypothesis [33–35] led to a power law velocity profile [36,37], in addition to the traditional log laws. Similar analyses were used to deduce a power law temperature profile [32], which was proposed to be equivalent to the log-law temperature profile for large Peclet numbers. Seena and Afzal [38] also studied the scaling properties of the intermediate layer in a fully developed turbulent channel flow by employing the method of matched asymptotic expansions. They proposed a half-defect velocity law and a half temperature defect law in association with the intermediate layer. Their prediction of Reynolds shear stress and Reynolds heat flux profiles in the intermediate layer show good agreement with available experimental and DNS data. Moreover, by assuming the existence of overlap layers Seena et al. [39] constructed a closure model that leads to a series of logarithmic functions of the mesolayer variable for Reynolds shear stress and Reynolds heat flux profiles.

Herein we take a different approach to study the scaling properties admitted by the mean thermal energy equation. This framework only relies on the magnitude ordering of the terms in the mean energy equation, and thus does not invoke additional assumptions or resort to the use of a closure model. Recent analyses of turbulent wall bounded flow for both pipe and channel [1,40–43] indicate that many of the statistical properties of these flows are similar, even though they possess different geometric configurations. Notably, analyses of the mean momentum equation can be directly employed to explore the underlying physics and scaling of the dependent variables in that equation. Wei et al. [1] introduced a generic first-principles framework to characterize the four layer regime in wall bounded flows, an extension of which leads to a mesoscaling of Reynolds shear stress [43] and mean velocity field [44] in turbulent channel flows. The limiting value of Reynolds number at which the four layer magnitude orderings are first established has been investigated for channel flows by Elsnab et al. [45]. However, the onset of four-layer regime for thermal field is not yet well characterized, as it is a function of both Reynolds and Prandtl numbers. In fact, as shown herein, a number of conditions depending on the magnitude of Reynolds and Prandtl numbers factor into determining the onset of the four-layer thermal structure.

An important observation obtained from the mean momentum balance theory [46,47] is the existence of a hierarchy of scaling layers with each having an analytically well-defined characteristic length. The conditions for logarithmic dependence of the mean velocity profile were explored by using this approach [48,49]. The analogous method was subsequently applied to channel flow heat transfer by Wei et al. [2]. This effort revealed a qualitative characterization of the four layer regions, Peclet number dependence of the scaling of temperature, and the conditions associated with the existence of the logarithmic mean temperature profile. However, a more comprehensive elucidation of the scaling behaviours of the mean energy equation is still lacking, and this motivates the present effort.

Multiscale analyses are used herein to clarify the scaling properties admitted by the mean energy equation. In order to describe mean flow structure properly, a length scale intermediate to the traditional inner and outer scales is necessary. According to the present theory, the transition from inner to outer scaling physically takes place owing to a balance breaking and exchange of the leading order heat transport mechanisms as a function of scale. This underlies the existence of an intermediate region between inner and outer layers (thermal mesolayer) where, in the mean, all terms in the energy equation are of equal order [2]. In order to gain a better understanding of the possibilities for generating invariant profiles of the mean temperature and turbulent heat flux, the current investigation exploits the properties of four distinct balance layers in a magnitude ordering and scaling analysis of the mean energy equation. The analyses primarily employ existing DNS data sets of Kawamura and co-workers [17,20,50].

2. Mean momentum layer structure

To provide a context for the heat transfer problem, it is useful to briefly review the four layer structure associated with the mean momentum balance. The relative magnitude of the terms in the Reynolds-averaged Navier–Stokes equations are used to define the layer properties. This fundamentally differs from the traditional four layer structure for turbulent channel flows [51–53]; namely the viscous sublayer ($y^+ = yu_\tau/\nu < 5$, where y is the wall-normal distance, ν is the kinematic viscosity and u_τ is the friction velocity), the buffer layer ($5 \leqslant y^+ \leqslant 30$), the inertial (or classical logarithmic layer, $30 \leqslant y^+ \lesssim 0.15Re_\tau$, where Re_τ is the Kármán number, $Re_\tau = u_\tau\delta/\nu$) and the outer boundary layer or wake layer ($0.15 \leqslant y/\delta \lesssim 1.0$). It also fundamentally differs from the structure proposed by Wosnik et al. [54]. They divided the flow into the main 'viscous sublayer', 'overlap' and 'outer' regions. The near-wall region, where $0 < y^+ < 30$, was composed of the linear viscous

sublayer and the buffer zone. The overlap region, where $30 \lesssim y^+ \lesssim 0.15Re_\tau$ is built of a mesolayer and the inertial sublayer. The viscous sublayer and overlap region constitute the inner region. The outer region extends from $0.15Re_\tau$ to the channel centerline. Another important observation from their work was that there might be an underlying layer which extended from near $y^+ = 30$ to approximately $y^+ = 300$ where the dissipative motions were not fully separated in scale from the energy containing motions. This region was related to what they called a mesolayer, following the same concepts of George and Castillo [26] for boundary layers.

By considering the relative magnitudes of the terms in the mean momentum equation, Wei et al. [1] rationally deduced a different four layer structure for wall-bounded turbulent flow. They observed from the available experimental and numerical data that three of these layers reflect the dominance of two out of the three dynamical effects in the mean momentum equation. But there exists another layer, where all three terms make non-negligible contributions to the overall balance. This leads to an identification of the dynamical balance characteristics of distinct physical layers from the mean momentum equation theory. Close to the wall, the first layer (layer I) is reflected by a nominal balance between mean pressure gradient and viscous stress gradient. This layer is similar to the traditional viscous sublayer whose thickness is $O(\nu/u_\tau)$. The next adjacent layer exists where the leading-order balance occurs between Reynolds stress gradient and viscous stress gradient. Layer III is the one where all three terms in the relevant mean momentum equation are of equal order. Within this layer, the zero crossing of the Reynolds stress gradient and its location play a significant role. The fourth layer represents a balance between the Reynolds stress gradient and the mean pressure gradient. Elsnab et al. [45] further pointed out that the four-layer structure and its order-of-magnitude scaling behaviours remain valid for all Kármán numbers above the transitional regime.

Klewicki et al. [49] explained the existence and properties of the layer hierarchy on the basis of the first-principles-based theory developed in [1,46,47,55]. They revealed an underlying hierarchy of scaling layers, and the conditions for a logarithmic mean velocity profile. These properties all stem from the mean momentum equation admitting an invariant form on each layer of the continuous layer hierarchy. This similar approach is also applicable to the mean thermal layer structure. However, the problem gets more complicated because of the extra governing parameter, the Prandtl number.

3. Mean thermal layer structure: traditional and four-layer description

Following the analogy between heat and momentum transfer, the common way to characterise the mean thermal layer regions is an inspection of the structure of the governing equations for energy and momentum. This analogy becomes exact if the Prandtl numbers are unity. Thus the thermal boundary layer for wall bounded turbulent flow can be divided into the classical four layer structure within two separate scaling regions through the observed properties of the mean temperature and turbulent heat flux profiles [3,4]. An inner thermal region close to the heated solid wall is composed of a molecular or conductive sublayer and thermal buffer layer, whereas an outer region commonly known as core thermal region extends to the centerline of the pipe or channel. The classical logarithmic layer and the outer layer constitute the outer thermal region. This picture also proposes the existence of an overlap region where both inner and outer representations are valid.

Using 'equilibrium similarity analysis', George and Castillo [26], Castillo and George [56], and Wang and Castillo [57] derived the temperature scaling for turbulent boundary layers. The mean structure they proposed is depicted in Fig. 1. The thermal overlap region (i.e., the common region between the inner and outer layers) has two sublayers namely convective sublayer with negligible conduction effect and thermal mesolayer where the conduction term has certain effects on the turbulent heat flux. Over the past century, this traditional four layer structure along with the similar depiction of the momentum field provided the basis for many researchers (e.g., [3,4]) to develop the mean temperature profiles valid within each thermal layer.

Wei et al. [2] developed a mean energy equation analysis analogous to that for the mean momentum equation [1]. As with momentum analysis, the relative magnitudes of the terms in the energy equation determine the underlying layer structure: layer I: molecular diffusion/mean advection balance layer, layer II: heat flux gradient balance layer, layer III: molecular diffusion/mean advection balance meso layer, layer IV: inertial/advection balance layer. Fig. 2 provides a schematic of the four layer thermal structure by examining the ratio of the heat flux gradients. Wei et al. [2] attempted to describe the scalings associated with thermal four layer structure using available DNS data. They introduced a new inner variable for thermal boundary layer based on the magnitude of centerline temperature and Peclet number. Here we extend their analysis by adopting a more general approach to clarify the existence of thermal layer properties.

In related analyses, Seena and Afzal [38] introduced a meso scaling theory of turbulent heat transfer in smooth and transitionally rough channel. Their theory was based on the mesolayer theory for turbulent flows developed by Afzal [31,58]. Similar to the three layer model for turbulent flow, Seena and Afzal [38] proposed that the fully developed turbulent heat transfer in a channel consists of three main layers: inner, intermediate and outer. They also proposed the existence of two overlap domains where $T(y)$ becomes logarithmic. Their inner thermal length scale is $\delta_{ti} = \alpha/u_\tau$ where α is the thermal diffusivity, and their outer scale is $\delta_{to} = \delta$, where δ is the channel half width. The thermal mesolayer scale δ_{tm} is the geometric mean of inner and outer length scales $\delta_{tm} = \sqrt{\delta_{ti}\delta_{to}} = \delta(PrRe_\tau)^{-1/2}$, where Pr is the Prandtl number. Their analyses indicated that the temperature profile in the mesolayer scale provides the half temperature defect law where mesolayer temperature is $T_m = (T_w + T_c)/2$ and T_w and T_c are the temperature on the wall and the axis of the channel respectively. Within the intermediate layer, they also proposed generalized logarithmic laws for temperature profiles in terms of the mesolayer variable using the method of matched asymptotic expansions. Moreover, Seena et al. [39] proposed a closure model of Reynolds heat flux

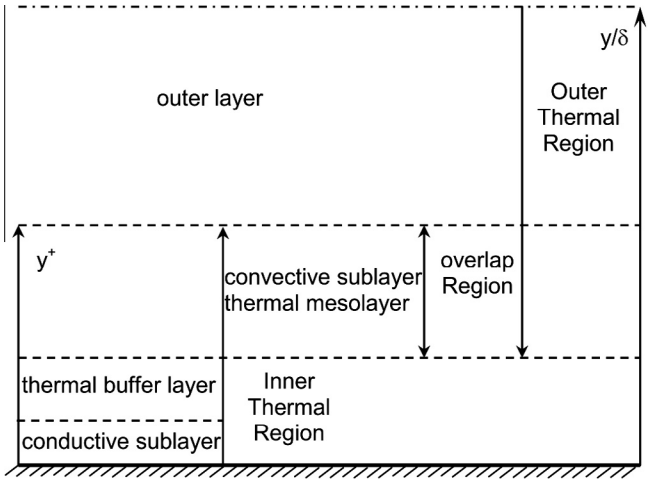

Fig. 1. Schematic of the mean temperature profile based layer structure.

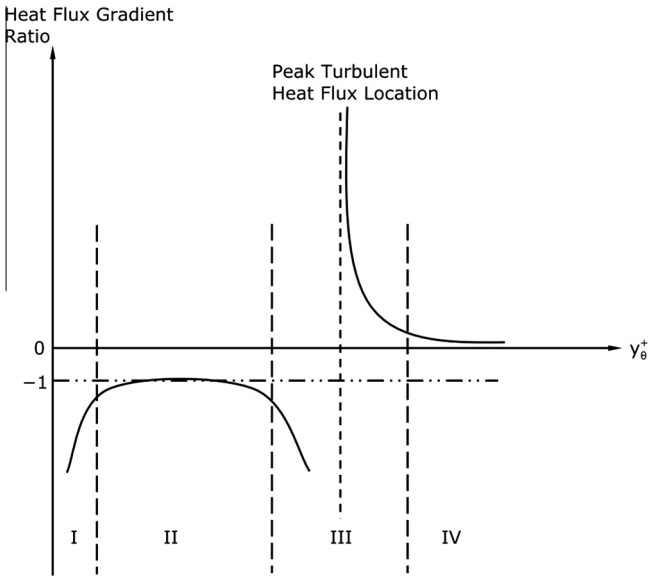

Fig. 2. Sketch of the four layers of turbulent heat transfer in canonical flows for one Peclet number; layer I is the molecular diffusion/mean advection balance layer, layer II is the heat flux gradient balance layer, layer III is the molecular diffusion/mean advection balance meso layer and layer IV is the inertial/advection balance layer. Note that the layer III is also called the balance breaking layer where the turbulent heat flux gradient crosses through zero.

as a function of a series of logarithmic functions in the mesolayer variable. Distinct from Afzal and co-workers, the present analyses do not assume overlap layers and do not employ asymptotic expansions.

The mean energy balance equation is governed by the balance between the molecular diffusion, turbulent transport and mean streamwise advection. Due to a balance breaking and exchange of these mechanisms, the intermediate region (thermal mesolayer) exists between inner and outer layers where, in the mean, all these three terms are nearly in balance. Finding the appropriate length scales that allow the construction of a self-consistent invariant form of the appropriate leading order equation on the inner, outer and intermediate domains is inherently a two parameter problem. Herein we present a systematic study that clarifies the nature of the underlying parameter dependencies.

4. Derivation of mathematical model

4.1. Mean energy balance equation

The present analysis begins with the appropriate form of the mean energy equation. The analysis considers statistically stationary, fully developed, incompressible, pressure driven turbulent flow and heat transfer in a two-dimensional channel. The fluid properties are assumed to be constant. Temperature is treated as a passive scalar.

The three-dimensional instantaneous energy balance equation for an incompressible flow with constant properties and negligible viscous heating is given by

$$\frac{\partial \tilde{T}}{\partial \tilde{t}} + \tilde{u}_x \frac{\partial \tilde{T}}{\partial x} + \tilde{u}_y \frac{\partial \tilde{T}}{\partial y} + \tilde{u}_z \frac{\partial \tilde{T}}{\partial z} = \alpha \left[\frac{\partial^2 \tilde{T}}{\partial x^2} + \frac{\partial^2 \tilde{T}}{\partial y^2} + \frac{\partial^2 \tilde{T}}{\partial z^2} \right], \tag{1}$$

where $\tilde{u}_x$, $\tilde{u}_y$ and $\tilde{u}_z$ are the instantaneous velocity components in the x, y and z directions, $\tilde{T}$ is the instantaneous temperature, $\tilde{t}$ is time and ρ is the mass density of fluid. The terms in the above energy balance equation are decomposed into their mean and fluctuating parts using:

$$\tilde{u}_x = U + u; \;\; \tilde{u}_y = V + v; \;\; \tilde{u}_z = W + w, \;\; \text{and} \;\; \tilde{T} = T + t, \tag{2}$$

where U, V, W are the mean velocity components in x, y and z directions, u, v, and w are the corresponding fluctuating velocity components, T is the mean temperature and t is the corresponding fluctuating temperature. The temporal average of the product ut, vt and wt are denoted by $\langle ut \rangle$, $\langle vt \rangle$ and $\langle wt \rangle$, respectively. The resulting time-averaged energy balance equation is

$$U\frac{\partial T}{\partial x} + V\frac{\partial T}{\partial y} + W\frac{\partial T}{\partial z} = \alpha \left[\frac{\partial^2 T}{\partial x^2} + \frac{\partial^2 T}{\partial y^2} + \frac{\partial^2 T}{\partial z^2} \right] - \frac{\partial \langle ut \rangle}{\partial x} - \frac{\partial \langle vt \rangle}{\partial y} - \frac{\partial \langle wt \rangle}{\partial z}. \tag{3}$$

For the given flow, (3) reduces to

$$U\frac{\partial T}{\partial x} = \alpha \left[\frac{\partial^2 T}{\partial x^2} + \frac{\partial^2 T}{\partial y^2} \right] - \frac{\partial \langle vt \rangle}{\partial y}. \tag{4}$$

In fully developed heat transfer, the mean temperature is a linearly increasing function of x and the rate of increase can be determined by applying an energy balance to a differential element of the channel. This yields

$$\frac{\partial T}{\partial x} = \frac{q_w}{\rho C_p U_b \delta}, \tag{5}$$

where, $q_w = k(\partial T/\partial y)_w$ is the heat flux applied at the upper and bottom walls, k is the thermal conductivity, C_p is the specific heat and $U_b = \frac{1}{\delta}\int_0^\delta U(y)dy$ is the bulk mean velocity. The right hand side of (5) is constant, and using the definition of Prandtl number, $Pr = \nu/\alpha$, the averaged energy balance equation becomes

$$\frac{q_w U}{\rho C_p U_b \delta} = \frac{\nu}{Pr}\frac{\partial^2 T}{\partial y^2} - \frac{\partial \langle vt \rangle}{\partial y}. \tag{6}$$

Eq. (6) contains two unknown functions, mean temperature T and turbulent heat flux $\langle vt \rangle$. These are the quantities of primary interest. The boundary conditions at the channel wall, $y = 0$, are

$$U = u = v = t = 0, \;\; \frac{\partial T}{\partial y} = \frac{q_w}{k}, \tag{7}$$

and at the centerline, $y = \delta$, are

$$\frac{\partial T}{\partial y} = \langle vt \rangle = 0. \tag{8}$$

4.2. Normalizations

The friction velocity u_τ, inner length for momentum, ν/u_τ, and outer length, δ, are often considered as the basic normalization parameters for turbulent flow problems. Moreover, the normalization parameters used herein for the heat transfer problem are the friction temperature $T_\tau = q_w/\rho C_p u_\tau$ and an inner normalized length $\nu Pr^{-b}/u_\tau$ generalized by considering a power law Prandtl number effect. In addition to these parameters, the non-dimensional temperature $\Theta^+ = (\langle T_w \rangle - T)/T_\tau$ gives (6) its convectional inner normalized form,

$$\frac{1}{Pr}\frac{d^2\Theta^+}{dy^{+2}} + \frac{dT_\theta^+}{dy^+} + \varepsilon^2 \frac{U^+}{U_b^+} = 0, \tag{9}$$

where $T_\theta^+ = -\langle vt \rangle^+$ is the inner normalized turbulent heat flux. The small parameter ε is defined by

$$\varepsilon = \frac{1}{\sqrt{\delta^+}}, \tag{10}$$

where $\delta^+ = u_\tau \delta/\nu$ is the Reynolds number (Kármán number), so that $\varepsilon \to 0$ as $\delta^+ \to \infty$. The outer normalized form of (6) is found by using

the channel half-width δ to normalize the wall normal distance $\eta = y/\delta$. This gives

$$\frac{\varepsilon^2}{Pr}\frac{d^2\Theta^+}{d\eta^2} + \frac{dT_\theta^+}{d\eta} + \frac{U^+}{U_b^+} = 0. \tag{11}$$

The boundary conditions at the channel wall, $y^+ = 0$, are

$$U^+ = \Theta^+ = T_\theta^+ = 0, \quad \frac{d\Theta^+}{dy^+} = Pr, \tag{12}$$

and at the centerline, $y^+ = \delta^+$, are

$$\frac{d\Theta^+}{dy^+} = T_\theta^+ = 0. \tag{13}$$

Both Pr and δ^+ play important roles in the following analysis. Eq. (9) implies a fully developed thermal field hence there is no dependence on axial direction. At sufficiently high Re_τ, U^+/U_b^+ is $O(1)$ for all values of y^+ values beyond the peak in the Reynolds shear stress, and in this region $U^+/U_b^+ \to 1$ as $\delta^+ \to \infty$. Note that the wall-normal distance is still normalised by the length scale of the viscous sublayer, ν/u_τ.

Wei et al. [2] developed an alternative normalized form of (6) by introducing the parameter σ which is a function of δ^+ and Peclet number $Pe_\tau = Pr\delta^+$, and is defined as

$$\sigma^2(\delta^+, Pe_\tau) = \max\left(\frac{\Theta^+}{Pr\delta^+}\right) = \frac{\Theta^+|_{\eta=1}}{Pe_\tau} = \frac{\Theta_m^+}{Pe_\tau}. \tag{14}$$

Given this, a new σ-dependent temperature variable ψ follows and is expressed as

$$\psi = \frac{\Theta^+}{Pe_\tau\sigma^2}. \tag{15}$$

This renders $\psi = O(1)$ near the channel center and $\sigma \ll 1$. The corresponding outer normalized form of (9) is

$$\sigma^2\frac{d^2\psi}{d\eta^2} + \frac{dT_\theta^+}{d\eta} + R(\eta) = 0, \tag{16}$$

where $R(\eta) = U^+/U_b^+$ is the scaled advection function. By employing the generic inner-outer variable relation, Wei et al. [2] defined a new inner scaled distance y_σ as

$$y_\sigma = \frac{\eta}{\sigma^2}, \tag{17}$$

which generates a scaled advection function $R_\sigma(y_\sigma) = R(\eta(y_\sigma)) = R(\sigma^2 y_\sigma)$. This yields a new 'inner' form of (6),

$$\frac{d^2\psi}{dy_\sigma^2} + \frac{dT_\theta^+}{dy_\sigma} + \sigma^2 R_\sigma(y_\sigma) = 0, \tag{18}$$

$$A + B + C = 0,$$

where the relationship between the inner and outer coordinates is given by (17). The boundary conditions on (18) are

$$\psi = T_\theta^+ = 0, \quad \frac{d\psi}{dy_\sigma}(0) = 1 \quad \text{at } y_\sigma = 0. \tag{19}$$

In the following analysis, we examine three alternative forms of (6), distinct from (18), in order to clarify the dependences on Pr. We introduce a new inner variable $y_\theta^+ = Pr^b y^+$. Its use yields three cases for (6).

Case I.

$$\frac{d^2\Theta^+}{dy_\theta^{+2}} + \frac{dT_\phi^+}{dy_\theta^+} + \phi^2 R_\theta(y_\theta^+) = 0, \tag{20}$$

$$A + B + C = 0,$$

where $T_\phi^+ = Pr^{1-b}T_\theta^+$ and the small parameter ϕ is defined by

$$\phi = \frac{1}{\sqrt{\delta^+ Pr^{2b-1}}}. \tag{21}$$

The thermal boundary conditions at the channel wall, $y_\theta^+ = 0$, are

$$\Theta^+ = 0, \quad \frac{d\Theta^+}{dy_\theta^+} = Pr^{1-b}. \tag{22}$$

Here Θ^+ is not scaled by Pr, and both the boundary condition and the advection term depend on Pr. If we consider $b = 1$, then the new inner scaled energy equation takes the form of the traditional inner Eq. (9).

Case II.

$$\frac{d^2\Phi^+}{dy_\theta^{+2}} + \frac{dT_\theta^+}{dy_\theta^+} + \phi^2 R_\theta(y_\theta^+) = 0, \tag{23}$$

$$A + B + C = 0,$$

where $\Phi^+ = Pr^{b-1}\Theta^+$ and the small parameter ϕ is defined by

$$\phi = \frac{1}{\sqrt{\delta^+ Pr^b}}. \tag{24}$$

The thermal boundary conditions at the channel wall, $y_\theta^+ = 0$, are

$$\Phi^+ = 0, \quad \frac{d\Phi^+}{dy_\theta^+} = 1. \tag{25}$$

Here T_θ^+ is not scaled by Pr, and nor are the boundary conditions at the wall. There is, however, a Prandtl number dependence in the advection term.

Case III.

$$\frac{d^2\Phi^+}{dy_\theta^{+2}} + \frac{dT_\phi^+}{dy_\theta^+} + \phi^2 R_\theta(y_\theta^+) = 0, \tag{26}$$

$$A + B + C = 0,$$

where $\Phi^+ = Pr^{2b-1}\Theta^+$, $T_\phi^+ = Pr^b T_\theta^+$ and the small parameter ϕ is defined by

$$\phi = \frac{1}{\sqrt{\delta^+}}. \tag{27}$$

The thermal boundary conditions at the channel wall are

$$\Phi^+ = 0, \quad \frac{d\Phi^+}{dy_\theta^+} = Pr^b. \tag{28}$$

Here there is no Pr dependence in the small parameter.

All three cases of above suggest that $1/\phi^2$ must be large enough to maintain a turbulent state for flow and heat transfer. Three distinct mechanisms are clearly apparent in Eqs. (18), (20), (23), (26): A = gradient of the molecular diffusion flux, B = gradient of the turbulent transport flux and C = mean streamwise advection.

5. Data sets

Herein we use the DNS data sets from Kawamura's group [17,20,50] for $0.025 \leqslant Pr \leqslant 10.0$ and $180 \leqslant Re_\tau \leqslant 1020$. Optimally, one would like to have a high Re_τ condition and then vary Pr. Owing to existing computational limitations, high Pr and high Re_τ are, however, not simultaneously possible. Thus, a single Kármán number near the onset of the four layer momentum structure ($Re_\tau = 180$) is selected to study Pr effects, see Fig. 3 [45]. The

domain size, number of grid points (N_x, N_y and N_z), spatial resolution, parameter ranges and symbol are shown in Table 1.

6. Establishment of thermal four layer regime

6.1. The heat flux gradient ratios

The relative orders of magnitude of terms A, B and C in Eqs. (18), (20), (23), (26) become distinct in four layers as $Re_\tau \to \infty$ and $Pr \to \infty$. One of the possibilities is that the three physical effects, in order of magnitude, balance. Otherwise two terms in Eqs. (18), (20), (23), (26) balance to leading order with the third much smaller. The ratio of any two terms exposes the leading order balance. At any fixed Prandtl number, the scaled advection function approaches a constant in the outer portion of the flow as Re_τ becomes large. This is similar to the behaviour of the mean advection function in the boundary layer [59].

Fig. 4 clarifies the onset of the four layer regime by examining the ratio of terms A/B. This figure shows that near the onset of the four layer regime for momentum ($Re_\tau \lesssim 180$), the thermal field exhibits a similar and discernible layer structure that depends on the magnitude of Prandtl number. Fig. 5 shows the existence of the four layer thermal structure for varying Re_τ and Pr. Different leading order balances organize on four distinct layers: layer I: $|C| \cong |A| \gg |B|$, layer II: $|A| \cong |B| \gg |C|$, layer III: $|A| \cong |B| \cong |C|$, layer IV: $|C| \cong |B| \gg |A|$. The data of Fig. 4 demonstrate that the balance between the dominating terms A and B smoothly develop the structure of Fig. 2. In fact, we are able to connect the transitional four-layer thermal regimes by determining the minimum values of the governing parameters at which the predominant characteristics of the thermal four-layer regime exist.

The data plotted in Fig. 4 are selected for $0.025 \leqslant Pr \leqslant 0.71$ and reveal that the heat flux gradient ratio attains very large negative values at low Pr. With increasing Pr, the ratio continually progress toward a plateau at -1. As explained by Wei et al. [2], the reason for such behaviour completely depends on the balance between the terms A and B. For example, at low Pr the molecular diffusion term A dominates over the turbulent term B across the whole layer. Moreover, the Reynolds heat flux gradient is crucial to the thermal energy balance in the region interior to the location of the peak heat flux. Note further that, the ratio plotted in Fig. 4 comes close to -1 in layer II with increasing Reynolds number for very low Prandtl number ($Pr = 0.025$). It is found, however, that the layer

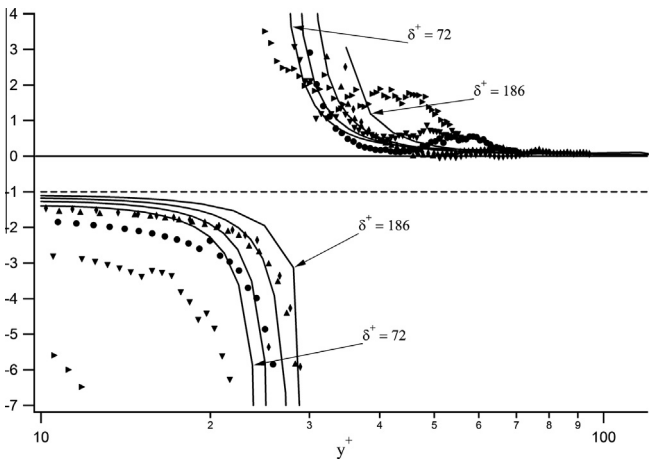

Fig. 3. Ratio of the gradient of the viscous stress to the gradient of the Reynolds stress for increasing δ^+ in the transitional regime. These data reveal the emergence of the four layer momentum field structure. This figure is adapted from Elsnab et al. [45].

IV ratio for the lowest Prandtl number retains non zero values all the way to the centerline even with increasing Reynolds number. This is consistent with an outer region influence of the molecular diffusion flux in the transitional heat transfer regime. When the Prandtl number is $Pr \geqslant 0.6$, there is a region (layer II) where the ratio approximately equals -1 and near-zero region in layer IV. Another important observation is that the -1 ratio region moves inward with increasing Prandtl number and decreasing Reynolds number.

6.2. Minimum Prandtl number of the four-layer regime

Establishment of thermal four-layer structure depends on the combined effects of Kármán and Prandtl number. As these parameters are varied, different routes to the four layer regime become apparent. There are two possibilities that are especially note worthy. One is the existence of the thermal four layer regime below the onset of the momentum four-layer regime ($Re_\tau < 180$). However, due to the lack of available DNS data in this range, it is not possible to examine this case. Hence we focus on the investigation of minimum Prandtl number in order to determine the existence of the thermal four-layer structure for a Re_τ at least near or above the onset of the four-layer regime for the momentum field.

Elsnab et al. [45] and later Klewicki et al. [48,59] used two primary criteria to determine the minimum Reynolds number at which the ordering of terms in the mean momentum equation are estimated to enter its four layer regime. The first criterion pertains to the ordering of terms in layers II and IV described relative to Fig. 2. The second requirement is to check the consistency of the layer thickness and the velocity increments across the layers documented in [48,59]. For turbulent heat transfer, the analogous criteria are applicable. Since the available data is within the range of Reynolds number for four-layer regime, our aim is to focus on Prandtl numbers for which the ordering of terms satisfy the thermal four-layer structure. The thermal layer scaling properties in terms of the layer width and temperature increments across the layers are at present, not known analytically. Thus, we concentrate on the minimum Prandtl number for the establishment of thermal four layer regime for $Re_\tau \gtrsim 180$.

Following Elsnab et al. [45], we assumed that both in layer II and IV, the smaller of the two dominant terms is ten times larger than the smallest term. For the lowest $Pr = 0.025$ when $Re_\tau = 1020$, neither layer II ($|B/C|_{max} \simeq 7.69$) nor layer IV ($|B/A|_{max} \simeq 1.82$) criterion is satisfied. Close examination of data for $Pr = 0.4$ and $Re_\tau = 180$ reveals that $|B/C|$ attains a maximum value of 12.6 in layer II, but $|B/A|_{max} \simeq 8.4$ in the inner part of layer IV. As a result, the requirement is satisfied only in layer II for this Pr. On the other hand, the heat flux gradient ratios barely satisfy the layer IV criterion at $Pr \simeq 0.6$, where the magnitude of the Reynolds heat flux gradient first attains 12.3 times the magnitude of the molecular diffusion flux gradient near the centre of layer IV. Similarly, the heat flux gradient ratio A/B in Fig. 4 rapidly attains a value in near -1 in layer II, though the molecular diffusion flux gradient does not become 10 times the value of the mean advection term until $Pr \simeq 0.4$. From these considerations, we conclude that the four layer thermal regime exists when $Pr \gtrsim 0.6$ at $Re_\tau \simeq 180$.

6.3. Properties of thermal four-layer regime

Fig. 5 displays mean energy balances for y_θ^+ as a function of b in the manner represented in Fig. 2. Detailed examination reveals the following. Layer I is a thin sublayer ($0 \leqslant y_\theta^+ \leqslant y_c$, where the value of y_c depends on the selection of b in $y_\theta^+ = Pr^b y^+$) in which the mean streamwise advection and the gradient of the molecular diffusion dominate the balance equation. The next layer is a region characterized by an increasingly exact balance between the molecular

Table 1
Summary of DNS database for turbulent heat transfer in channel flow. Data is adopted from the DNS database of Kawamura's group [17,20,50] at http://murasun.me.noda.tus.ac.jp/turbulence/poi/poi.html.

Re_τ	Pr	Pe_τ	L_x/δ	N_x	N_y	N_z	Δx^+	Δy^+	Δz^+	Symbol
180	0.025	4.5	12.8	256	128	256	9.0	0.20–5.90	4.50	▼
180	0.05	9	6.4	128	66	128	9.0	0.4–11.5	4.50	♠
180	0.1	18	6.4	128	66	128	9.0	0.4–11.5	4.50	♥
180	0.2	36	6.4	128	66	128	9.0	0.4–11.5	4.50	♣
180	0.4	72	6.4	128	66	128	9.0	0.4–11.5	4.50	★
180	0.6	108	6.4	128	66	128	9.0	0.4–11.5	4.50	✷
180	0.71	127.8	6.4	1024	480	512	1.1	0.05–0.97	1.1	•
180	1.0	180	6.4	1024	480	512	1.1	0.05–0.97	1.1	▶
180	2.0	360	6.4	1024	480	512	1.1	0.05–0.97	1.1	◆
180	5.0	900	6.4	256	128	256	4.50	0.20–5.90	2.25	▲
180	7.0	1260	6.4	2048	480	512	0.56	0.05–0.97	1.1	◀
180	10.0	1800	6.4	2048	480	512	0.56	0.05–0.97	1.1	■
395	0.025	9.875	12.8	512	192	512	9.88	0.15–6.52	4.94	▽
395	0.71	280.45	6.4	2048	480	512	1.2	0.11–2.1	2.5	○
395	1.0	395	6.4	2048	480	512	1.2	0.11–2.1	2.5	▷
395	2.0	790	6.4	2048	480	512	1.2	0.11–2.1	2.5	◇
395	5.0	1975	6.4	2048	480	512	1.2	0.11–2.1	2.5	△
395	7.0	2765	6.4	2048	480	512	1.2	0.11–2.1	2.5	◁
395	10.0	3950	6.4	2048	120	512	1.2	0.11–2.1	2.5	□
640	0.025	16	12.8	1024	256	1024	8.00	0.15–8.02	4.00	ø
640	0.71	454.4	12.8	1024	256	1024	8.00	0.15–8.02	4.00	⊗
1020	0.025	25.5	12.8	2048	448	1536	6.38	0.15–7.32	4.25	©
1020	0.71	724.2	12.8	2048	448	1536	6.38	0.15–7.32	4.25	⊕

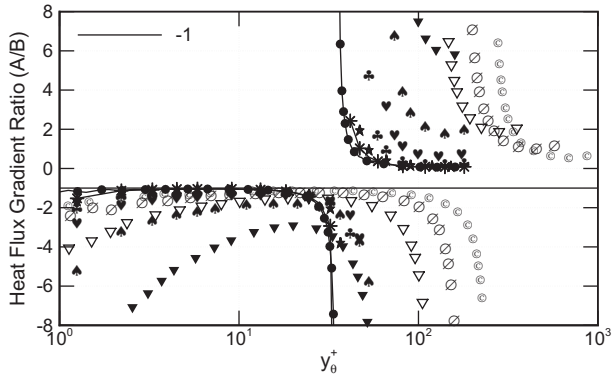

Fig. 4. Ratio of the gradient of the molecular diffusion flux to the gradient of the turbulent transport flux (A/B). Symbol shapes for DNS data are given in Table 1. The solid lines show data for $Pr \geqslant 0.6$. The wall normal distance y_θ^+ is chosen as y^+ for the case at $b = 0$. Data sets are from the DNS database of Kawamura's group [17,20,50].

diffusion flux and turbulent heat flux gradients (layer II). This behaviour is similar to the mean momentum balance where the viscous force and turbulent inertia constitute the leading order balance. The thickness of the heat flux gradient balance layer shows a definite Reynolds and Prandtl number dependence which extends more into the traditionally accepted logarithmic region of the mean temperature profile at sufficiently large Reynolds and Prandtl number. Near the location of peak turbulent heat flux, molecular diffusion and mean advection are nearly in balance again (layer III). In layer III, there is a balance breaking and exchange process in which all the terms in the mean heat equation are important. In this layer, the turbulent heat flux gradient changes sign and the molecular diffusion flux gradient becomes much smaller than either the turbulent heat flux gradient or the streamwise mean advection gradient terms. By the end of layer III the gradients of turbulent heat flux and the streamwise mean advection are leading order, which defines layer IV. It is clear here that this layer structure establishes a definite departure from the layer structure of Fig. 1.

A closer look at Fig. 5 reveals some interesting parameter dependencies of the thermal four-layer structure. The open symbols in this figure represent data for higher Reynolds number ($Re_\tau \geqslant 395$), whereas the closed symbols indicate $Re_\tau = 180$. The balance breaking and exchange of forces characteristic of layer III in the momentum equation is known to become distinct with increasing Reynolds number. The same feature also appears in the thermal four-layer regime with increasing Reynolds and Prandtl numbers. However, when the viscous length scale used to represent the layer structure (Fig. 5(a) at $b = 0$), the effects of Re_τ and Pr on the heat flux gradient ratio act opposite to each other. With the introduction of thermal length scale ($b \neq 0$), the Prandtl number starts showing similar influence as Reynolds number and finally for $b = 1$, the inner scaled variable takes the Pr-dependent form $y_\theta^+ = Pry^+$ which clearly contains the effect of Reynolds and Prandtl number (Fig. 5). The initial opposite nature of Pr causes one to suspect that the profiles of Fig. 5 will become invariant for a certain value of b.

Although Wei et al. [2] described the characteristic properties of the thermal four-layer structure, they did not determine the scaling behaviours associated with the widths of these layers and temperature increments across them. As observed in Fig. 5, the inner length strongly influences these layer widths and temperature increments. Herein, we aim to clarify the factors involved in solving this task. A principal intention is to mathematically and physically describe the mean heat transfer properties of the four layer regime with respect to the balance breaking and exchange mechanism in layer III, as this describes the transition from the inner to intermediate length.

7. Inner and outer scaling of turbulent heat transfer

Fully developed thermal statistics in turbulent flow typically use inner and outer normalizations analogous to those used to describe the mean streamwise velocity profile. This inner and outer scaling of temperature can be expressed by the following relation (e.g., [14,15,20]),

$$\Theta^+ = f_i(y^+), \tag{29}$$

$$\Theta_c^+ - \Theta^+ = f_o(\eta), \tag{30}$$

where f_i and f_o are assumed to be universal functions and the subscript c represents the centreline value. Eq. (29) is referred as the

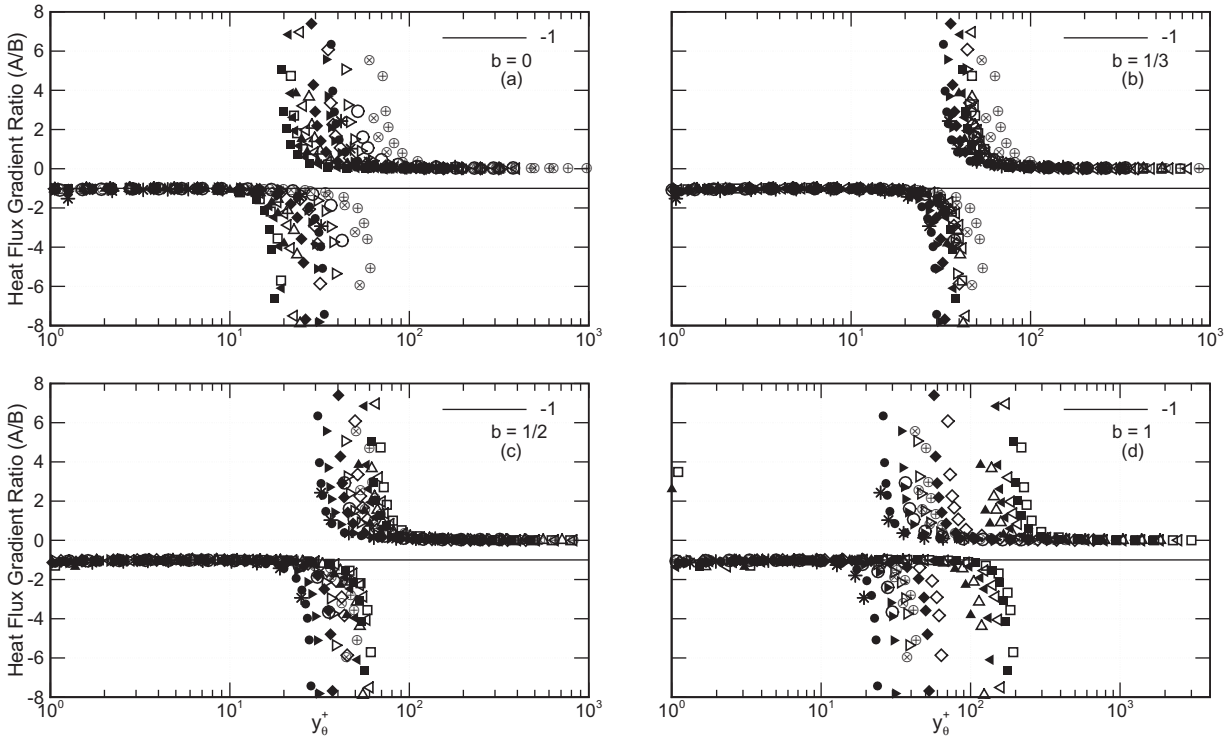

Fig. 5. Heat flux gradient ratio (A/B) of fully developed turbulent heat transfer in a channel for $Pr \geqslant 0.6$. (a)–(d) Results from the present proposal of (20), (23), (26) for different value of b. Data sets are from the DNS database of Kawamura's group [17,20,50].

law of the wall for the mean temperature and (30) is called the temperature defect law. Fig. 6 shows the inner and outer-normalised mean temperature and turbulent heat flux profiles. The present DNS data reveal that (29) generally fails to produce invariant temperature or heat flux profiles for varying Reynolds and Prandtl numbers. Outer normalization, however, convincingly scales both the mean temperature and the turbulent heat flux profiles over a large outer domain. Interestingly, neither of these normalizations scale the data near the peak heat flux. It is evident from Fig. 6(d) that the outer normalised maximum turbulent heat flux location moves inward with increasing Reynolds and Prandtl numbers and gradually the peak value increases and apparently approaches one. For large Reynolds and Prandtl numbers, when the value of ε^2/Pr becomes very small and $R(\eta)$ is $O(1)$, the $O(\varepsilon^2/Pr)$ term in the outer normalised mean energy balance (10) may be neglected, leaving

$$\frac{dT^+_\theta}{d\eta} + R(\eta) = 0, \tag{31}$$

and integrated using the boundary condition to obtain

$$T^+_\theta(\eta) = -\int_1^\eta R(\eta)d\eta = 1 - \eta, \tag{32}$$

results a linear variation of the heat flux independent of Reynolds and Prandtl numbers. This condition satisfies in the domain where, from (10), the mean streamwise advection and turbulent transport flux gradient comprise the leading order balance. The inner normalized mean temperature profiles also fail to merge (see Fig. 6(a)) due to dependences on both Re_τ and Pr. An apparent reason for this is that the conventional normalization does not explicitly include the effect of Prandtl number. This results in poor characterisation of the mean temperature profiles under different diffusive transport conditions. On the other hand, the outer scaling of mean temperature as shown in Fig. 6(b) merges temperature profiles in the outer layer (say, $\eta > 0.2$).

Fig. 6(a) depicts the inner scaling profile considered from the present proposal for case I at $b = 0$ and this type of inner scaling for mean temperature has been proposed by many researchers [7,10–14,16–20,23–25]. Moreover, cases II and III for $b = 0$ represent the inner scaled heat flux profile shown in Fig. 6(c) which was also previously shown [7,12–16,18]. Due to the limitation of this kind of inner scaling, an alternate was proposed based on a Taylor series expansion of the mean temperature profile. This results in a Pr-dependent normalized mean temperature, Θ^+/Pr, as successfully adopted by Abe et al. [10] and Kawamura et al. [17,18]. Fig. 7(a) shows the alternate inner scaling of mean temperature which is described by cases II and III for $b = 0$. This alternate scaling supports an extension of the conductive sublayer up to $y^+ \simeq 5$. Like the mean temperature, the turbulent heat fluxes can also be normalised by Prandtl number to account for the near wall effect. Kawamura et al. [7,17,18] deduced this alternate scaling for the heat flux profile based on the series expansion of fluctuating components of velocity and temperature, see in Fig. 7(b).

The mean temperature and turbulent heat flux profiles derived from the formulation of Wei et al. [2] are shown in Fig. 8. Their inner normalization yields a convincing invariance for the mean temperature. The heat flux profile, however, exhibits a small but discernible Reynolds number effect for $y_\sigma < 1.0$. Here the closed symbols indicating $Re_\tau = 180$, seem to merge for varying Pr. The open symbols ($Re_\tau > 180$), however, exhibit variations. This scaling will be discussed further in Section 9.

Here we have considered case I to show the effect of the coefficient b on the inner scaling of mean temperature and turbulent heat flux. For the reasons explained in Section 9, we omit a detailed presentation of the other cases. The parameter b varies from 0 to 1 showing the dependence of Prandtl number on the thermal length scale. The influence of Reynolds number on both the mean temperature and heat flux is accounted for by using the traditional viscous length scale. However, only the thermal length scale considers the effect of both Reynolds and Prandtl numbers, and this effect is

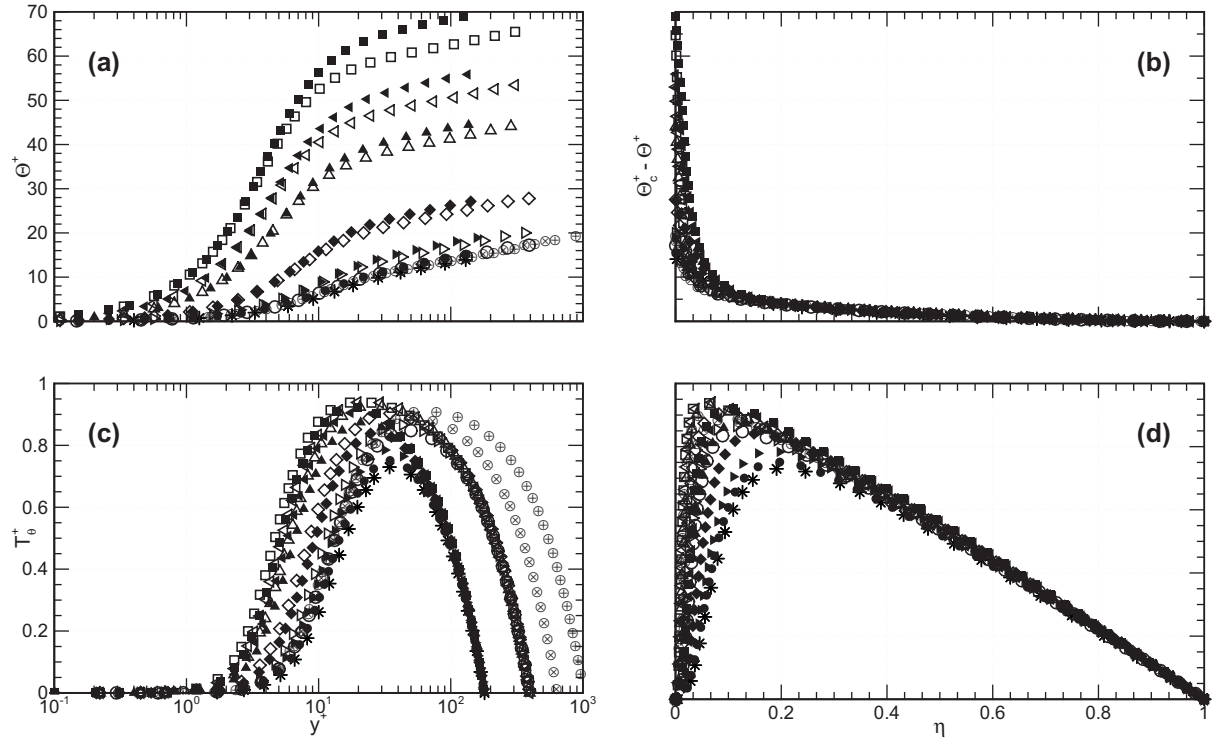

Fig. 6. Traditional inner and outer scaling of mean temperature and turbulent heat flux for fully developed turbulent heat transfer in a channel. (a) Inner scaling of mean temperature, (b) outer scaling of mean temperature (temperature defect law), (c) inner scaling of turbulent heat flux and (d) outer scaling of heat flux. Data sets are as for Fig. 5.

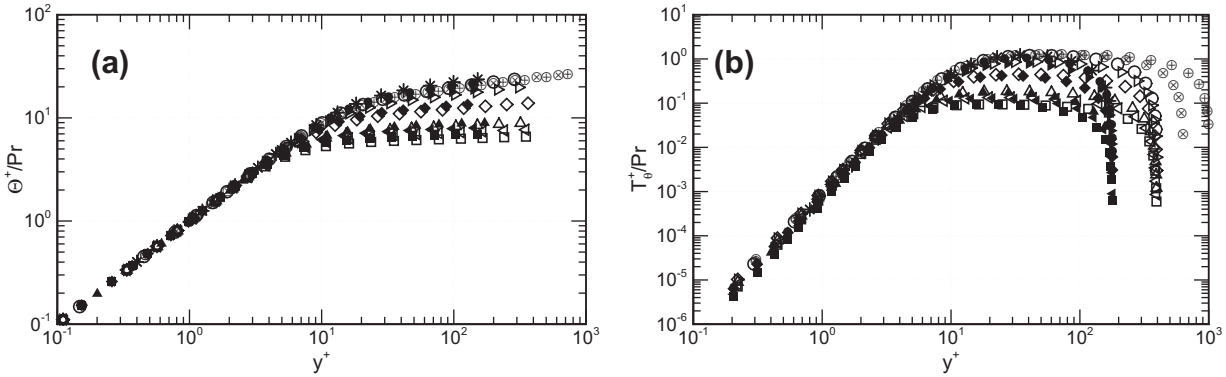

Fig. 7. Alternate inner scaling (log–log) of (a) mean temperature and (b) turbulent heat flux. Data sets are as for Fig. 5.

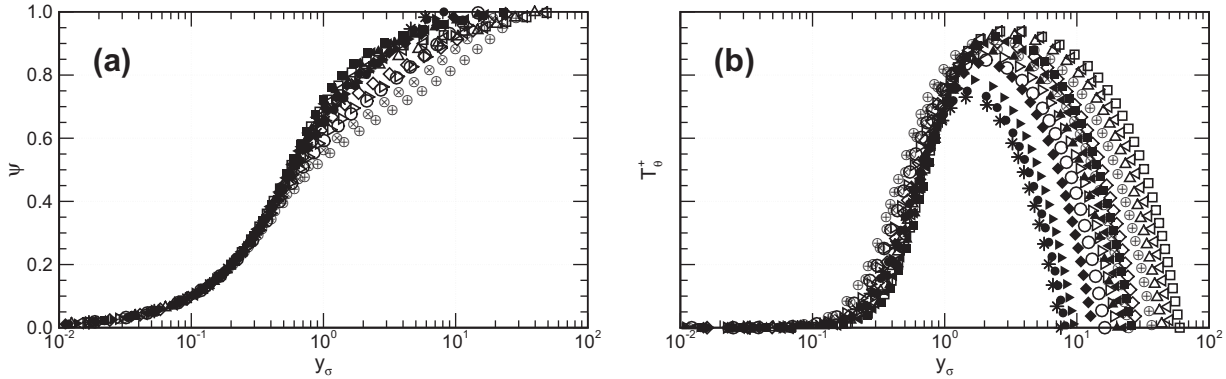

Fig. 8. Inner scaling of (a) mean temperature and (b) turbulent heat flux following Wei et al. [2]. Data sets are as for Fig. 5.

exemplified in Figs. 9 and 10. When $b = 1$, one recovers the alternate scaling of Fig. 7(a). On the other hand, the inner scaled turbulent heat flux fails to match near the wall, as the expression of heat flux profile changes with b. With increasing b, the limit of turbulent heat flux approaches unity, although the near wall profile shows dependencies on both Re_τ and Pr (Fig. 10(d)). Thus, in summary, the introduction of b on the thermal length scale allows us to determine the condition under which the inner normalization yields the invariant profiles of mean temperature and turbulent heat flux near the wall.

8. Intermediate length scaling

The inner and outer flow subdomains are characterized by the distance variables y_σ in (18) or y_θ^+ in (20), (23), (26) and η respectively. The theory of Wei et al. [2] indicates that these subdomains are connected by the continuous layer hierarchy discussed at the end of Section 3. Layer III in Fig. 2 is the consequence of this underlying layer hierarchy. In wall-bounded turbulent heat transfer, the intermediate layer (layer III) is accurately described as the central layer on the hierarchy. This layer is centered about the peak in the turbulent heat flux T_θ^+ [1,31]. We present rescaled versions of the thermal energy equation that reflect and thus clarify this description for the three cases considered.

Following Wei et al. [2], rescaling is most easily accomplished for the differentials dy_σ and dT_θ^+,

$$dy_\sigma = \pi_1 d\hat{y}_\sigma, \quad dT_\theta^+ = \pi_2 dT_\theta, \quad d\psi = d\hat{\psi}, \tag{33}$$

where $\hat{\psi}$ and T_θ are the rescaled $O(1)$ functions of $\hat{y}_\sigma$ and σ and π_1 and π_2 are scaling factors to be determined. The terms in (18) transform as,

$$\frac{d^2\psi}{dy_\sigma^2} = \frac{1}{\pi_1^2}\frac{d^2\hat{\psi}}{d\hat{y}_\sigma^2}, \quad \frac{dT_\theta^+}{dy_\sigma} = \frac{\pi_2}{\pi_1}\frac{dT_\theta}{d\hat{y}_\sigma}. \tag{34}$$

We now require that the derivatives on the right of (34), namely $d^2\hat{\psi}/d\hat{y}_\sigma^2$ and $dT_\theta^+/d\hat{y}_\sigma$, be $O(1)$ quantities. By this requirement, the orders of magnitude of both terms on the right, namely $1/\pi_1^2$ and π_2/π_1, must match the third term in (18), namely $\sigma^2 : \pi_1^{-2} = \pi_2/\pi_1 = \sigma^2$. This is only possible if $\pi_2 = \sigma$, $\pi_1 = \sigma^{-1}$. Thus from (33)

$$dy_\sigma = \sigma^{-1} d\hat{y}_\sigma, \quad dT_\theta^+ = \sigma dT_\theta. \tag{35}$$

Integrating (35) gives two integration constants which are conveniently chosen to be $y_{\sigma m}$ and $T_{\theta m}^+$, as they are the values of y_σ and T_θ^+ where $\hat{y}_\sigma = 0$ and $T_\theta = 0$. The result is

$$y_\sigma = y_{\sigma m} + \sigma^{-1}\hat{y}_\sigma, \quad T_\theta^+ = T_{\theta m}^+ + \sigma T_\theta, \tag{36}$$

where the quantities with subscript m are the values of those variables at the maximum point $y_{\sigma m}$ of T_θ^+. The meso-scaled variables now become

$$\hat{y}_\sigma = \sigma(y_\sigma - y_{\sigma m}), \quad T_\theta = (1/\sigma)(T_\theta^+ - T_{\theta m}^+), \quad \hat{\psi} = \psi - \psi_m, \tag{37}$$

where $y_{\sigma m}$ and $T_{\theta m}$ are the peak turbulent heat flux location and value, respectively, and ψ_m is the value of normalised mean temperature at $y_{\sigma m}$. Normalization of the mean energy equation according to these variables results in the invariant equation,

$$\frac{d^2\hat{\psi}}{d\hat{y}_\sigma^2} + \frac{d\hat{T}_\theta}{d\hat{y}_\sigma} + 1 = 0, \tag{38}$$

in which all terms are $O(1)$. Here we note that $dT_\theta^+/d\eta$ equates to $dT_\theta/d\hat{y}_\sigma$. This indicates that the intermediate scaling melds seamlessly into the outer scaling, and thus will be applicable from interior to y_m^+ to the channel center.

Similarly, the three alternative forms of the inner normalised energy equations (20), (23), (26) yield

Case I.

$$\hat{y} = \sqrt{\frac{Pr}{\delta^+}}(y^+ - y_m^+), \tag{39}$$

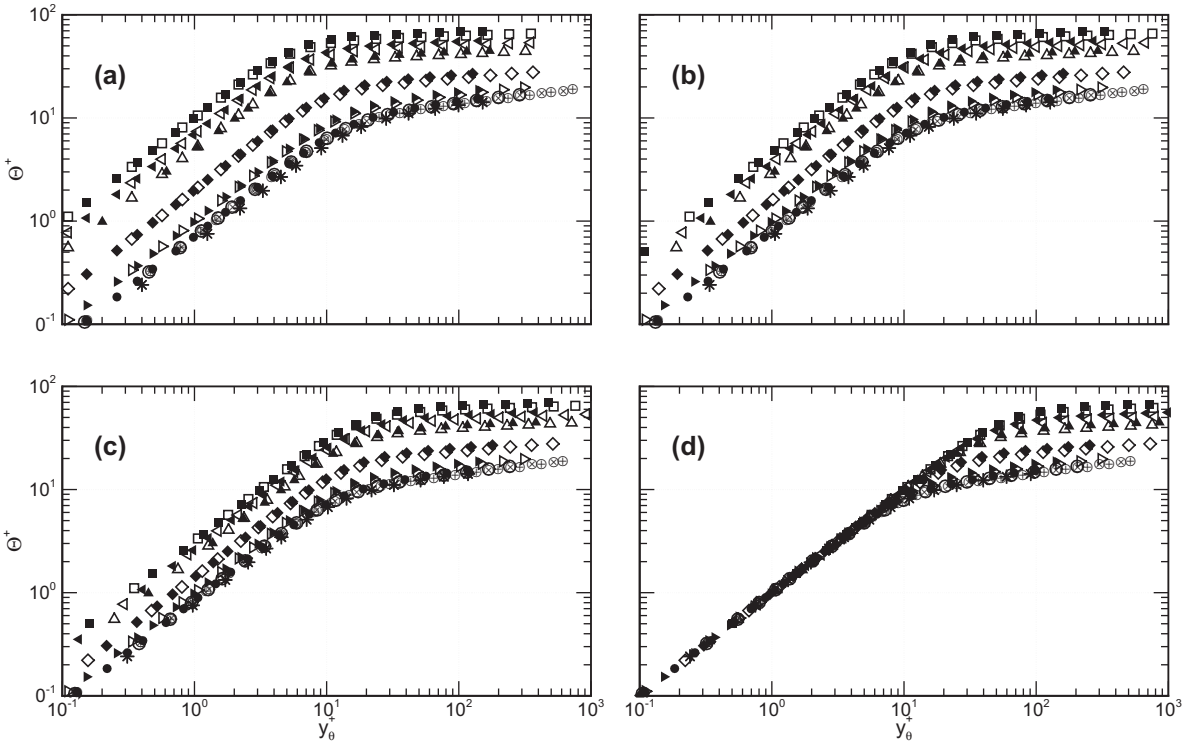

Fig. 9. Inner normalizations of mean temperature for Case I of Eq. (20). (a) $b = 0$, (b) $b = 1/3$, (c) $b = 1/2$ and (d) $b = 1$. Data sets are as for Fig. 5.

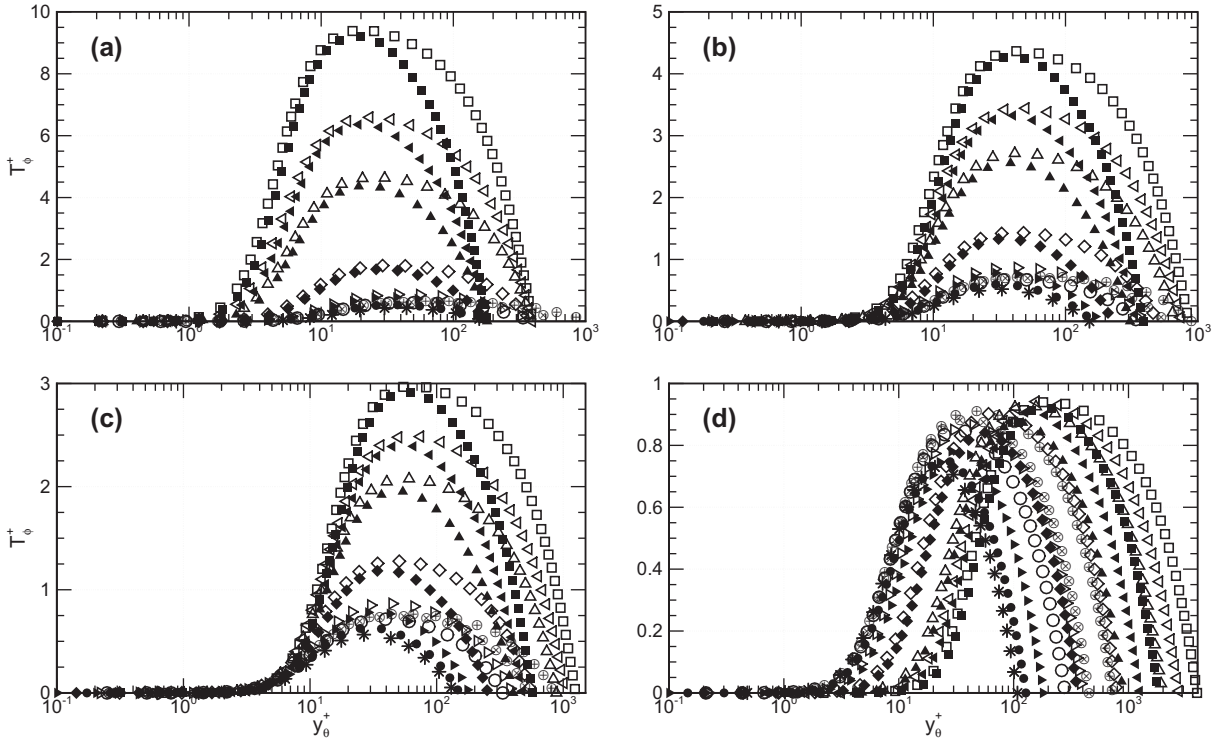

Fig. 10. Inner normalizations of turbulent heat flux for Case I of Eq. (20). (a) $b = 0$, (b) $b = 1/3$, (c) $b = 1/2$ and (d) $b = 1$. Data sets are as for Fig. 5.

$$\hat{T}_\phi = \sqrt{\delta^+ Pr}\left(T^+_\theta - T^+_{\theta m}\right), \tag{40}$$

$$\hat{\Theta} = \left(\Theta^+ - \Theta^+_m\right). \tag{41}$$

Note that these meso-scaled variables are independent of the coefficient b.

Case II.

$$\hat{y} = \sqrt{\frac{Pr^b}{\delta^+}}\left(y^+ - y^+_m\right), \tag{42}$$

$$\hat{T}_\phi = \sqrt{\delta^+ Pr^b}\left(T^+_\theta - T^+_{\theta m}\right), \tag{43}$$

$$\hat{\Theta} = Pr^{b-1}\left(\Theta^+ - \Theta^+_m\right). \tag{44}$$

If we consider $b = 1$, then all these meso-scaled variables become the same as case I and (23) takes the form of case I (20).

Case III.

$$\hat{y} = \sqrt{\frac{Pr^{2b}}{\delta^+}}\left(y^+ - y^+_m\right), \tag{45}$$

$$\hat{T}_\phi = \sqrt{\delta^+ Pr^{2b}}\left(T^+_\theta - T^+_{\theta m}\right), \tag{46}$$

$$\hat{\Theta} = Pr^{2b-1}\left(\Theta^+ - \Theta^+_m\right). \tag{47}$$

A similar situation as case II for $b = 1$ will happen if we consider $b = 1/2$ for case III. From this we conclude that case I yields a universal form of the intermediate scaling of (23). This intermediate form is derivable from the other cases and recovers the form proposed by Seena and Afzal [38]. Using these meso-scaled variables, the mean energy equation takes the parameter-free form as follows:

$$\frac{d^2\hat{\Theta}}{d\hat{y}^2} + \frac{dT_\phi}{d\hat{y}} + 1 = 0, \tag{48}$$

where all scaled terms have values that are $O(1)$. As now discussed, however, the pure Peclet number dependence of case I has yet to be reconciled with Pr dependent inner scaling discussed previously.

9. Discussion of implications

Fig. 11 shows the mesoscaling of the mean temperature and turbulent heat flux profiles for case I. All of the profiles convincingly merge to a single curve. This scaling for turbulent heat flux extends from inside the peak in T^+_θ to a zone very near the centerline. At a minimum, the mesoscaling should be valid over an $O(1)$ $\Delta\hat{y}$ domain, surrounding $y^+_m(\hat{y} = T_\phi = 0)$. The outer normalization of mean temperature and turbulent heat flux show invariant profiles away from the wall, and hence as noted above the intermediate normalization also scales these data. The mesoscaling does not hold very near the wall, as this is where inner scaling is expected to hold. This behaviour is also similar to the mesoscaling of Reynolds shear stress in the momentum field as explained by Wei et al. [1]. The matched asymptotic expansions analysis of Seena and Afzal [38] also reveals the similar meso-scaled profiles of the mean temperature and turbulent heat flux. The main feature of this case is that it does not depend on the choice of thermal length scale, which is a strong function of the coefficient b. But without having any proper inner scaled thermal heat flux limits the applicability of this approach. This is clarified further below by considering the properties of the layer hierarchy.

Cases II and III also show the same meso-scaled profiles of the mean temperature and turbulent heat flux as shown in Fig. 11 for $b = 1$ and $b = 1/2$ respectively. Other choices of b in these two cases fail to produce invariant temperature profiles. On the

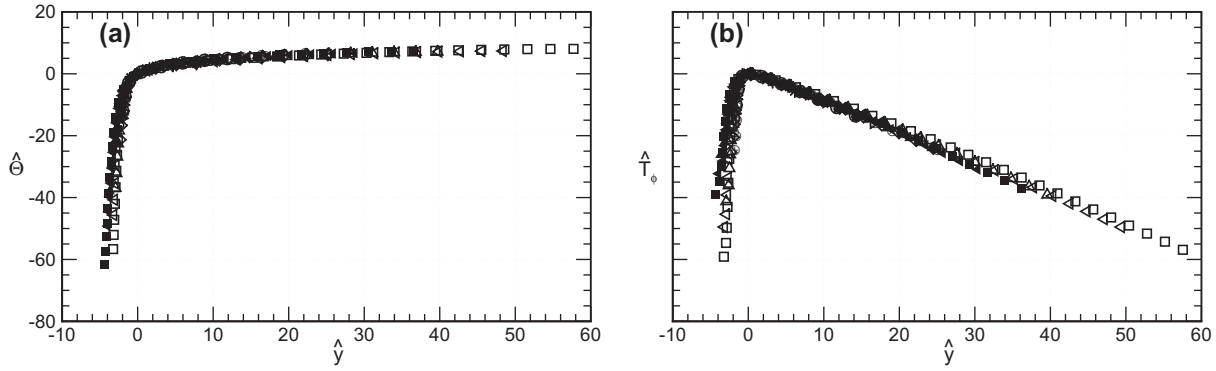

Fig. 11. Mesoscaling of (a) mean temperature and (b) turbulent heat flux for Case I. Data sets are as for Fig. 5.

other hand, the meso-scaled heat flux profiles can always be made invariant by choosing the appropriate value of b in the other cases. The existing theory proposed by Wei et al. [2] also faces a similar limitation. Their results are depicted in Fig. 12. As mentioned before, the meso-scaled temperature fails to merge from y_m^+ and into the outer region. On the other hand, the inner normalized temperature of Wei et al. [2] (Fig. 8) melds smoothly into the meso-scaling of Fig. 12. A thorough investigation of the inner normalised energy equation reveals that the normalised temperature function is most difficult to scale, even though the leading order balance of terms is known. The similarity between the normalised U^+ and Θ^+ profiles allow them to generate the invariant meso-scaled profiles both theoretically and quantitatively. However, any other normalization of the mean temperature profile (Θ^+, e.g., for ψ or Φ) results in a non-invariant profile of the meso-scaled variables.

The existence of the underlying invariant form of the mean thermal energy equation (38) or (48) reveals the self-similar heat transfer mechanisms from layer to layer with each having a distinct characteristic length. As a whole, these scaling layers are called as the L_γ hierarchy where L refers to the family layers on the hierarchy, and the subscript γ reflects the properties of the layer hierarchy. Namely, that the decay rate of the turbulent heat flux gradient establishes the width of each layer [2]. This inner

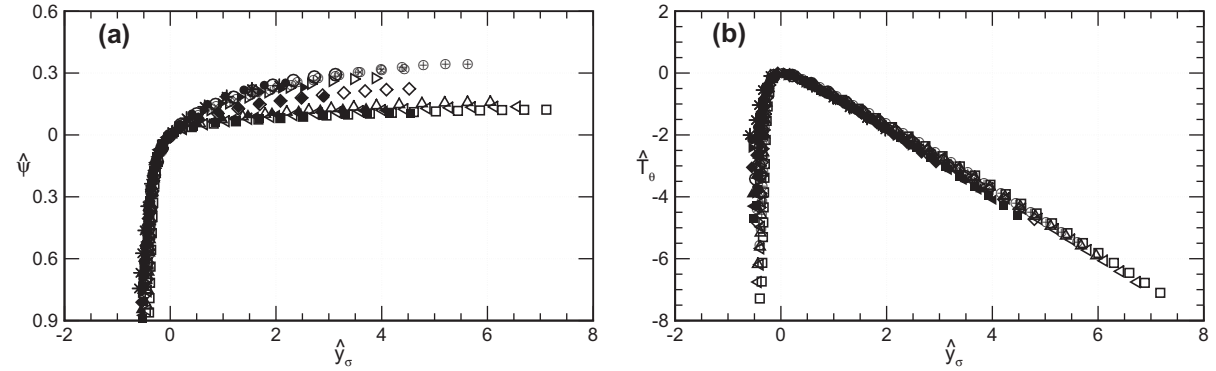

Fig. 12. Mesoscaling of (a) mean temperature and (b) turbulent heat flux following Wei et al. [2]. Data sets are as for Fig. 5.

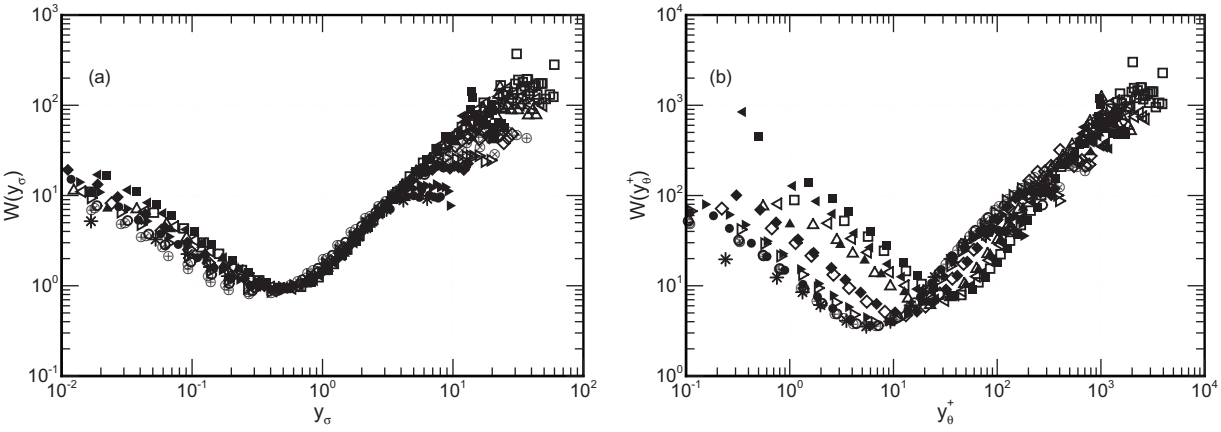

Fig. 13. Layer width distribution of the L_γ hierarchy for heat transfer in turbulent channel flow. (a) Formulation based on Wei et al. [2] and (b) Case I for $b = 1$. Data sets are as for Fig. 5.

normalized length distribution, W, accounts for the width of each L_γ as a function of y_θ^+. The layers on this hierarchy have increasing width with distance from the wall, with the first layer starting near the wall and the last layer ending near the centerline. Using the theory developed by Wei et al. [2], one can compute the layer width distribution, $W(y_\sigma)$, which effectively depends upon the decay rate of term B in (18) across the hierarchy. Namely,

$$W(y_\sigma) = O(\gamma^{-1/2}), \tag{49}$$

where the parameter γ can be evaluated as

$$\gamma = \frac{dT_\theta^+}{dy_\sigma} + \sigma^2 R_\sigma(y_\sigma). \tag{50}$$

The introduction of the new inner scale y_σ allows one to determine how the scaling approach effectively satisfies the layer hierarchy requirement with increasing Reynolds and Prandtl numbers. The mean momentum balance theory indicates that a linear $W(y^+)$ profile (exact or approximate) is required for the existence of a logarithmic mean velocity profile [49]. The same is applicable to the mean thermal energy balance relative to the development of a logarithmic mean temperature profile, and the evolution of the $W(y_\sigma)$ profiles is shown in Fig. 13(a) for the existing channel flow DNS data. The same theory also allows one to compute the layer width distributions, $W(y_\theta^+)$ under the normalization of case I and this is illustrated in Fig. 13(b). The remarkable finding here is that while both of the W distributions of Fig. 13 develop an approximately (emerging) linear W distribution, this W distribution is nearly invariant under the formulation of Wei et al. [2], but exhibits clear variations for the case I formulation.

10. Conclusions

The scaling properties of mean thermal energy balance equation for turbulent heat transfer in a channel have been investigated with the aid of existing DNS data. A generalized framework was employed. This allowed the relative influences of Re and Pr on the construction of invariant forms of the equation to be explored. Only one meso-normalization was found that accurately scaled both mean temperature and turbulent heat flux irrespective of the variations in Reynolds and Prandtl numbers. The derived meso-scaling (pure Pe) applied to both the turbulent heat flux and the mean temperature serves to merge the various data profiles to a single curve over a range of distances from the wall that extends from interior to the peak heat flux to the channel center line. This scaling characteristics exhibits similarity to the Reynolds stress at high Reynolds number. Unlike the momentum analysis, the proposed scaling approach fails to display the correct profile of the layer hierarchy associated with the intermediate normalization. The framework underlying the pure Peclet number scaling fails to yield viable inner scaling. Physically this may be because this framework does not automatically embrace the differential rates of heat and momentum transport in the region where the molecular diffusion is dominant.

Acknowledgements

The authors gratefully acknowledge the financial support of the Australian Research Council and the computational resources provided by a Victorian Life Sciences Computation Initiative (VLSCI) grant on its Peak Computing Facility at the University of Melbourne, an initiative of the Victorian Government. We wish to thank Dr. H. Abe for providing us turbulent heat transfer data ($Re_\tau = 1020$, $Pr = 0.025$).

References

[1] T. Wei, P. Fife, J. Klewicki, P. McMurtry, Properties of the mean momentum balance in turbulent boundary layer, pipe and channel flows, J. Fluid Mech. 522 (2005) 303–327.
[2] T. Wei, P. Fife, J. Klewicki, P. McMurtry, Scaling Heat Transfer in Fully Developed Turbulent Channel Flow, Int. J. Heat Mass Transfer 48 (2005) 5284–5296.
[3] R. Gowen, J. Smith, The effect of the Prandtl number on temperature profiles for heat transfer in turbulent pipe flow, Chem. Eng. Sci. 22 (1967) 1701–1711.
[4] B. Kader, Temperature and concentration profiles in fully turbulent boundary layers, Int. J. Heat Mass Transfer 24 (1981) 1541–1544.
[5] X. Wang, L. Castillo, G. Araya, Temperature Scalings and Profiles in Forced Convection Turbulent Boundary Layers, Journal of Heat Transfer 130 (2) 021701.
[6] M. Dhotre, J. Joshi, CFD Simulation of Heat Transfer in Turbulent Pipe Flow, Ind. Eng. Chem. Res. 43 (2004) 2816–2829.
[7] H. Kawamura, H. Abe, Y. Matsuo, DNS of Turbulent Heat Transfer in Channel Flow with Respect to Reynolds and Prandtl Number Effects, Int. J. Heat Fluid Flow 20 (1999) 196–207.
[8] S. Satake, T. Kunugi, R. Himeno, High Reynolds number computation for turbulent Heat Transfer in a pipe flow, in: High Performance Computing, Third International Symposium, Tokyo, Japan, 514–523, 2000.
[9] L. Redjem-Saad, M. Ould-Rouiss, G. Lauriat, Direct numerical simulation of turbulent heat transfer in pipe flows: Effect of Prandtl number, Int. J. Heat Fluid Flow 28 (5) (2007) 847–861.
[10] H. Abe, H. Kawamura, Y. Matsuo, DNS of Turbulent Heat Transfer in Channel Flow: Near-wall Turbulence Quantities, in: 13th Australasian Fluid Mechanics Conference, Melbourne, Australia, 849–852, 1998.
[11] H. Abe, H. Kawamura, Y. Matsuo, Surface heat-flux fluctuations in a turbulent channel flow up to Re_τ = 1020 with Pr = 0.025 and 0.71, Int. J. Heat Fluid Flow 25 (3) (2004) 404–419.
[12] N. Kasagi, Y. Ohtsubo, Direct Numerical Simulation of Low Prandtl Number Thermal Field in a Turbulent Channel Flow, vol. 8, Springer, Berlin, 1993, pp. 97–119.
[13] N. Kasagi, T. Tomita, K. Kuroda, Direct numerical simulation of passive scalar field in a turbulent channel flow, Trans. ASME J. Heat Transfer 114 (1992) 598606.
[14] H. Kawamura, H. Abe, DNS of turbulent scalar transport in a channel flow up to $Re_\tau = 640$ with $Pr = 0.025$ and 0.71, in: Seventh TRA Conference, Seoul Nat'l Univ., Seoul, Korea, 2002, pp. 65–79.
[15] H. Kawamura, H. Abe, Y. Matsuo, Very large-scale structures observed in DNS of turbulent channel flow with passive scalar transport, in: 15th Australasian Fluid Mechanics Conference, Sydney, Australia, 2004.
[16] H. Kawamura, H. Abe, K. Shingai, DNS of turbulence and heat transport in a channel flow with different Reynolds and Prandtl numbers and boundary conditions, in: Y. Nagano, K. Hanjalić, T. Tsuji (Eds.), Third International Symposium on Turbulence, Heat and Mass Transfer, 2000, pp. 15–32.
[17] H. Kawamura, K. Ohsaka, H. Abe, K. Yamamoto, DNS of turbulent heat transfer in channel flow with low to medium-high Prandtl number fluid, Int. J. Heat Fluid Flow 19 (5) (1998) 482–491.
[18] H. Kawamura, K. Ohsaka, K. Yamamoto, DNS of turbulent heat transfer in channel flow with low to medium-high Prandtl number Fluid, in: 11th Symposium Turbulent Shear Flows, vol. 1, Grenoble, 1997, pp. 8.7–8.12.
[19] J. Kim, P. Moin, Transport of Passive Scalars in a Turbulent Channel Flow, vol. VI, Springer-Verlag, 1989, pp. 85–96.
[20] M. Kozuka, Y. Seki, H. Kawamura, DNS of turbulent heat transfer in a channel flow with a high spatial resolution, Int. J. Heat Fluid Flow 30 (3) (2009) 514–524.
[21] M. Piller, E. Nobile, T.J. Hanratty, DNS study of turbulent transport at low Prandtl numbers in a channel flow, J. Fluid Mech. 458 (2002) 419–441.
[22] S. Saha, C. Chin, H. Blackbun, A. Ooi, The influence of pipe length on thermal statistics computed from DNS of turbuelnt heat transfer, Int. J. Heat Fluid Flow 32 (2011) 1083–1097.
[23] Y. Seki, K. Iwamoto, H. Kawamura, Prandtl number effect on turbulence quantities through high spatial resolution DNS of turbulent heat transfer in a channel flow, in: chap. Fifth International Symposium on Turbulence, Heat and Mass Transfer, Dubrovnik, Croatia, 2006, pp. 301–304.
[24] T. Tsukahara, Y. Seki, H. Kawamura, D. Tochio, DNS of turbulent heat transfer in a channel flow at very low Reynolds numbers, in: 1st International Forum on Heat Transfer, Kyoto, Japan, 2004, pp. 195–196.
[25] Y. Yamamoto, T. Kunugi, Y. Tsuji, Effects of very-large scale structures in a high-Reynolds turbulent channel flow on medium-high Prandtl number heat transfer (2009) 1–7.
[26] W.K. George, L. Castillo, Zero-pressure-gradient turbulent boundary layer, Appl. Mech. Rev. 50 (12) (1997) 689–729.
[27] S.W. Churchill, C. Chan, Turbulent flow in channels in terms of turbulent shear and normal stresses, AIChE J. 41 (12) (1995) 2513–2521.
[28] S.W. Churchill, B. Yu, Y. Kawaguchi, The accuracy and parametric sensitivity of algebraic models for turbulent flow and convection, Int. J. Heat Mass Transfer 48 (25-26) (2005) 5488–5503.
[29] P.M. Le, D.V. Papavassiliou, On temperature prediction at low Re turbulent flows using the Churchill turbulent heat flux correlation, Int. J. Heat Mass Transfer 49 (19-20) (2006) 3681–3690.

[30] N. Marati, J. Davoudi, C.M. Casciola, B. Eckhardt, Mean profiles for a passive scalar in wall-bounded flows from symmetry analysis, J. Turbulence 7 (2006) 61.
[31] N. Afzal, Fully developed turbulent flow in a pipe: An intermediate layer, Arch. Appl. Mech. (Ingenieur-Archiv) 52 (1982) 355–377.
[32] A. Seena, N. Afzal, Power law velocity and temperature profiles in a fully developed turbulent channel flow, J. Heat Transfer 130 (2008) 091701.
[33] A. Isakson, On the formula for the velocity distribution near walls, Tech. Phys. USSR. IV (1937) 155–159.
[34] A. Kolmogorov, The local structure of turbulence in incompressible viscous fluid for very large Reynolds numbers, in: Proceedings of the Royal Society, London, Ser. A, vol. 434 (1890), 1991, pp. 9–13.
[35] C. Millikan, A critical discussion of turbulent flow in channels and circular tubes, in: J. den Hartog, H. Peters (Eds.), 5th International Congress for Applied Mechanics, Wiley/Chapman and Hall, New York, London, 1938, pp. 386–392.
[36] N. Afzal, A. Seena, A. Bushra, Power law turbulent velocity profile in transitional rough pipes, J. Fluids Eng. 128 (3) (2006) 548–558.
[37] N. Afzal, A. Seena, A. Bushra, Power law velocity profile in fully developed turbulent pipe and channel flows, J. Hydraul. Eng. 133 (9) (2007) 1080–1086.
[38] A. Seena, N. Afzal, Intermediate scaling of turbulent momentum and heat transfer in a transitional rough channel, J. Heat Transfer 130 (2008) 031701.
[39] A. Seena, A. Bushra, N. Afzal, Logarithmic expansions for Reynolds shear stress and reynolds heat flux in a turbulent channel flow, ASME J. Heat Transfer 130 (2008) 094501.
[40] J.P. Monty, N. Hutchins, H.C.H. Ng, I. Marusic, M.S. Chong, A comparison of turbulent pipe, channel and boundary layer flows, J. Fluid Mech. 632 (2009) 431–442.
[41] J.P. Monty, J.A. Stewart, R.C. Williams, M.S. Chong, Large-scale features in turbulent pipe and channel flows, J. Fluid Mech. 589 (2007) 147–156.
[42] H. Ng, J. Monty, N. Hutchins, M. Chong, I. Marusic, Comparison of turbulent channel and pipe flows with varying Reynolds number, Exp. Fluids 51 (2011) 1261–1281.
[43] T. Wei, P. McMurtry, J. Klewicki, P. Fife, Mesoscaling of Reynolds shear stress in turbulent channel and pipe flows, AIAA J. 43 (11) (2005) 2350–2353.
[44] T. Wei, P. Fife, J. Klewicki, On scaling the mean momentum balance and its solutions in turbulent Couette–Poiseuille flow, J. Fluid Mech. 573 (2007) 371–398.
[45] J. Elsnab, J. Klewicki, D. Maynes, T. Ameel, Mean dynamics of transitional channel flow, J. Fluid Mech. 678 (2011) 451–481.
[46] P. Fife, J. Klewicki, P. McMurtry, T. Wei, Multiscaling in the presence of indeterminacy: wall-induced turbulence, Multiscale Model. Simul. 4 (3) (2005) 936–959.
[47] P. Fife, T. Wei, J. Klewicki, P. McMurtry, Stress gradient balance layers and scale hierarchies in wall-bounded turbulent flows, J. Fluid Mech. 532 (2005) 165–189.
[48] J. Klewicki, C. Chin, H. Blackburn, A. Ooi, I. Marusic, Emergence of the four layer dynamical regime in turbulent pipe flow, Phys. Fluids 24 (2012) 045107.
[49] J. Klewicki, P. Fife, T. Wei, On the logarithmic mean profile, J. Fluid Mech. 638 (2009) 73–93.
[50] Y. Seki, H. Kawamura, DNS of turbulent heat transfer in a channel flow with a varying streamwisely thermal boundary condition, Heat Transfer – Asian Res. 35 (4) (2006) 265–278.
[51] S.B. Pope, Turbulent Flows, Cambridge University Press, Cambridge, UK, 2000.
[52] H. Tennekes, J.L. Lumley, A First Course in Turbulence, MIT Press, Cambridge, MA, 1972.
[53] A.A. Townsend, The Structure of Turbulent Shear Flow, Cambridge University Press, Cambridge, UK, 1980.
[54] M. Wosnik, L. Castillo, W.K. George, A theory for turbulent pipe and channel flows, J. Fluid Mech. 421 (2000) 115–145.
[55] P. Fife, J. Klewicki, T. Wei, Time averaging in turbulence settings may reveal an infinite hierarchy of length scales, J. Discr. Contin. Dyn. Syst. 24 (3) (2009) 781–807.
[56] L. Castillo, W.K. George, Similarity analysis for turbulent boundary layer with pressure gradient: outer flow, AIAA J. 39 (1) (2001) 41–47.
[57] X. Wang, L. Castillo, Asymptotic solutions in forced convection turbulent boundary layers, J. Turbulence 4 (2003) N6.
[58] N. Afzal, Mesolayer theory for turbulent flows, AIAA J. 22 (3) (1984) 437–439.
[59] J. Klewicki, R. Ebner, X. Wu, Mean dynamics of transitional boundary-layer flow, J. Fluid Mech. 682 (2011) 617–651.